Geophysical Journal International

Geophys. J. Int. (2010) doi: 10.1111/j.1365-246X.2010.04784.x

GJI Geodynamics and tectonics

Contemporary deformation and stressing rates in Southern Alaska

Syed Tabrez Ali* and Andrew M. Freed

Department of Earth and Atmospheric Sciences, Purdue University, 550 Stadium Mall Dr., West Lafayette, IN 47907, USA. E-mail: stali@geology.wisc.edu

Accepted 2010 August 18. Received 2010 August 1; in original form 2009 November 7

SUMMARY

The subduction of the Pacific Plate beneath North America induces broad scale stressing of the Alaskan crust that has led to the development of the highest mountains in North America, the highest slip rates along some of the longest strike-slip faults on Earth, and widespread seismicity that includes the 1964 M9.2 Alaska earthquake, the second largest ever recorded. These features are a consequence of deformation associated with three primary processes, interseismic loading due to relative plate motions, large earthquakes and post-seismic processes. How these mechanisms contribute to the evolution of stress in the Alaskan crust is not well understood. Here we use observed contemporary surface velocities to constrain 2-D and 3-D viscoelastic numerical models of relative Pacific/North American plate motions, coseismic slip associated with the 1964 (M9.2) megathrust event and strike-slip earthquakes on the transform boundary in 1949 (M8.1), 1958 (M7.8) and 1972 (M7.6) (the four largest events prior to the 2002 M7.9 Denali quake), viscoelastic relaxation following these events, and afterslip, to gain insight into how these processes are shaping Alaska today. Results suggest that interseismic deformation and on-going post-seismic deformation following the 1964 earthquake both contribute significantly to the GPS measured contemporary velocity field. Viscoelastic relaxation associated with a mantle with a viscosity of $\sim 10^{19}$ Pa s is required to explain southerly directed velocities that are observed in the Cook Inlet region to well north of the Denali fault. Results also suggest that subduction of the Pacific Plate leads to a broad zone of deformation with high stressing rates concentrated in a band that lies several hundred kilometres from the plate boundary, coeval with the inboard location of the maximum locking depth of the megathrust. Interseismic deformation and stressing rates remain high further inland across the Yakutat microplate, where flat subduction extends the width of the locked plate interface. Calculations show that post-seismic relaxation following the large strike-slip events serves to reload these rupture surfaces while relieving stress on the eastern Denali Fault. Post-seismic relaxation following the 1964 earthquake combined with coseismic stress changes, promoted the triggering of the 2002 Denali quake. Calculations also suggest that over the past 50 years high stress has accumulated on part of the thrust interface to the west and east of the 1964 rupture surface and along the Queen-Charlotte Fault to the south of the 1949 rupture surface.

Key words: Seismic cycle; Transient deformation; Earthquake interaction, forecasting, and prediction; Continental margins: convergent; Rheology: crust and lithosphere.

1 INTRODUCTION

Few regions on Earth show the large-scale consequences of subduction as well as those observed in central and southern Alaska (Fig. 1). This area is characterized by rapid uplift of the Alaska, Wrangell and St. Elias mountain ranges, the highest in North America; high slip rates (up to 50 mm yr^{-1}) along some of the largest (>1000 km) strike-slip faults on Earth, such as the Queen Charlotte-Fairweather and Denali fault system; and most importantly from a hazard standpoint, widespread seismicity, including the 1964 M9.2 Alaska quake, the second largest earthquake ever recorded (Kanamori 1977), and the 2002 M7.9 Denali earthquake, the largest earthquake to occur within the North American continent in the past century (Eberhart-Phillips *et al.* 2003).

The timing and spatial extent of large earthquakes is a function of the evolution of stress in the upper crust. Knowledge of stressing rates is a powerful tool for assessing seismic hazards, as it cannot only be used to understand past events, but also to predict where

*Now at: Department of Geoscience, University of Wisconsin, 1215 W. Dayton St., Madison, WI 53706, USA.

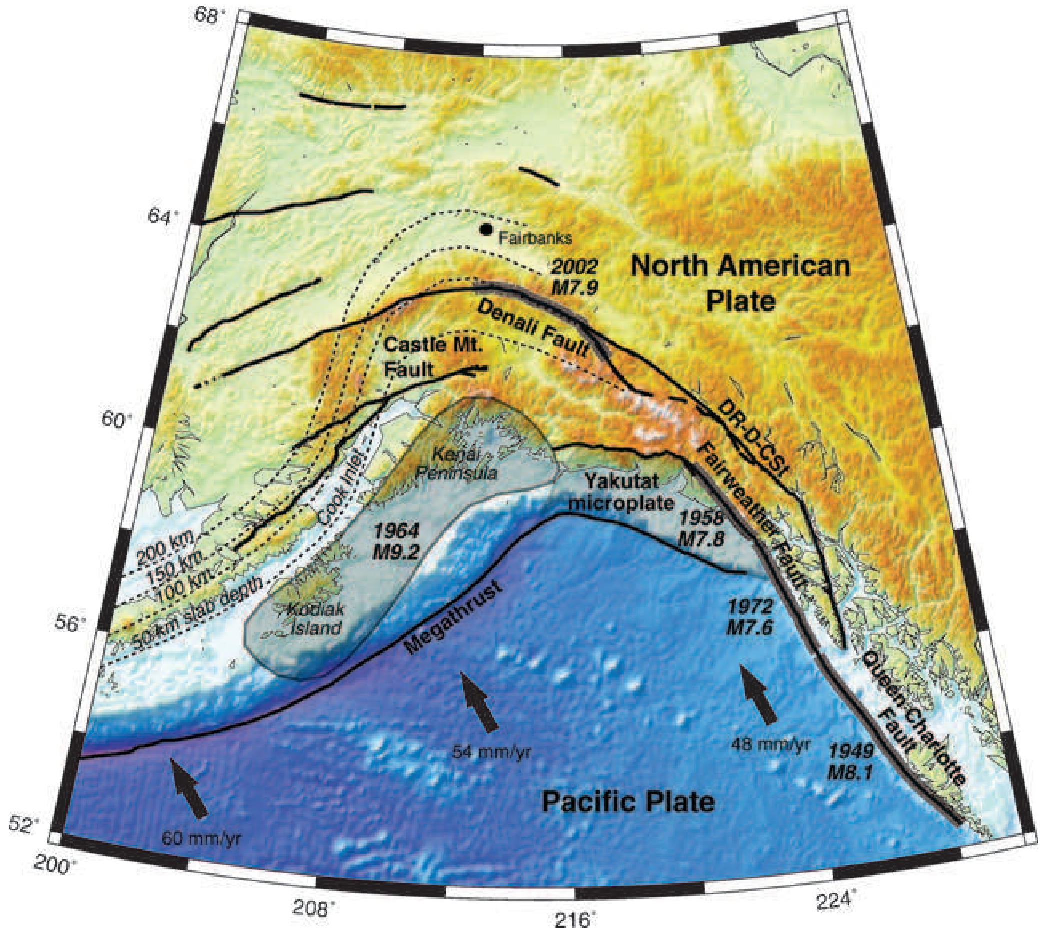

Figure 1. Map showing tectonic setting of Southern Alaska and surrounding region. Pacific slab depth contours shown as grey dashed lines. The rupture surfaces of the five earthquakes considered in this study are shown as grey lines/regions (see Table 1, for references). The Yakutat microplate is also shown in grey. Pacific Plate velocities are based after DeMets *et al.* (1994). DR–D–CSt, Duke River–Dalton–Chatham Strait Fault.

future earthquakes are likely to occur. Regional stressing rates vary greatly within the earthquake cycle. In the interseismic period the crust responds primarily elastically to plate motions, earthquakes then relieve these stresses through a process of permanent deformation (fault slip), then post-seismic viscoelastic relaxation transfers coseismic stresses from the hot lower crust and upper mantle to the seismogenic upper crust, leading to transient stressing rates that can take decades to decay back to interseismic levels.

Contemporary stressing rates can be constrained (in part) by observations of surface velocities. Comprehensive GPS observations made between 1997 and 2002 (Freymueller *et al.* 2008) have illuminated the contemporary velocity field of Southern Alaska (Fig. 2) prior to disruption of this field by the 2002 M7.9 Denali earthquake (Eberhart-Phillips *et al.* 2003; Freed *et al.* 2006a). Most of the observed velocities in the region trend northwestwards, coinciding with the general direction of the Pacific Plate convergence. However, a number of stations in the Cook Inlet area (just north of the vicinity of the 1964 rupture surface), as well as further inland near Fairbanks and beyond, show velocity vectors that trend southeastwards. These velocities have generally been attributed to on-going transient processes associated with 1964 Alaska quake, including post-seismic relaxation and afterslip or a combination of both (Zweck *et al.* 2002; Cohen & Freymueller 2004; Suito & Freymueller 2009). A similar phenomenon is currently observed in association with the 1960 M9.5 Great Chilean earthquake (e.g. Khazaradze *et al.* 2002). In addition to the 1964 earthquake, the contemporary velocity field may also be influenced by several strike-slip earthquakes that occurred on the Queen-Charlotte and Fairweather Faults in 1949 (M8.1), 1958 (M7.8) and 1972 (M7.6) (Fig. 1) (Nishenko & Jacob 1990), although previous analysis of the relative influence of various magnitude earthquakes in southern California (Freed *et al.* 2007) and northeastern Caribbean (Ali *et al.* 2008) would suggest that the influence of these events on the current velocity field and stress state of the region should be minimal compared to the much larger 1964 quake.

This work is motivated by several earlier studies of Alaskan tectonics. Bufe (2006) modelled interseismic deformation in Alaska using 3-D elastic models based on the motion of the subducting Pacific Plate in conjunction with a locked interface. This analysis, however, assumed that velocities that deviated from the direction of plate convergence (north–northwest) were not due to transient post-seismic processes, but instead due to long-term motion on other faults, specifically motion of a circular Wrangellian block defined by the Denali Fault to the north and the Fairweather and Queen-Charlotte faults to the east (Stout & Chase 1980). Bufe (2006) applied constant slip on these faults below a depth of 15 km, generating rotational shear of this block that enabled the model to explain a limited set of GPS observations that showed westward motion south of the Denali Fault and southerly motion in the Cook Inlet region. Such a model assumes that the contemporary velocity field

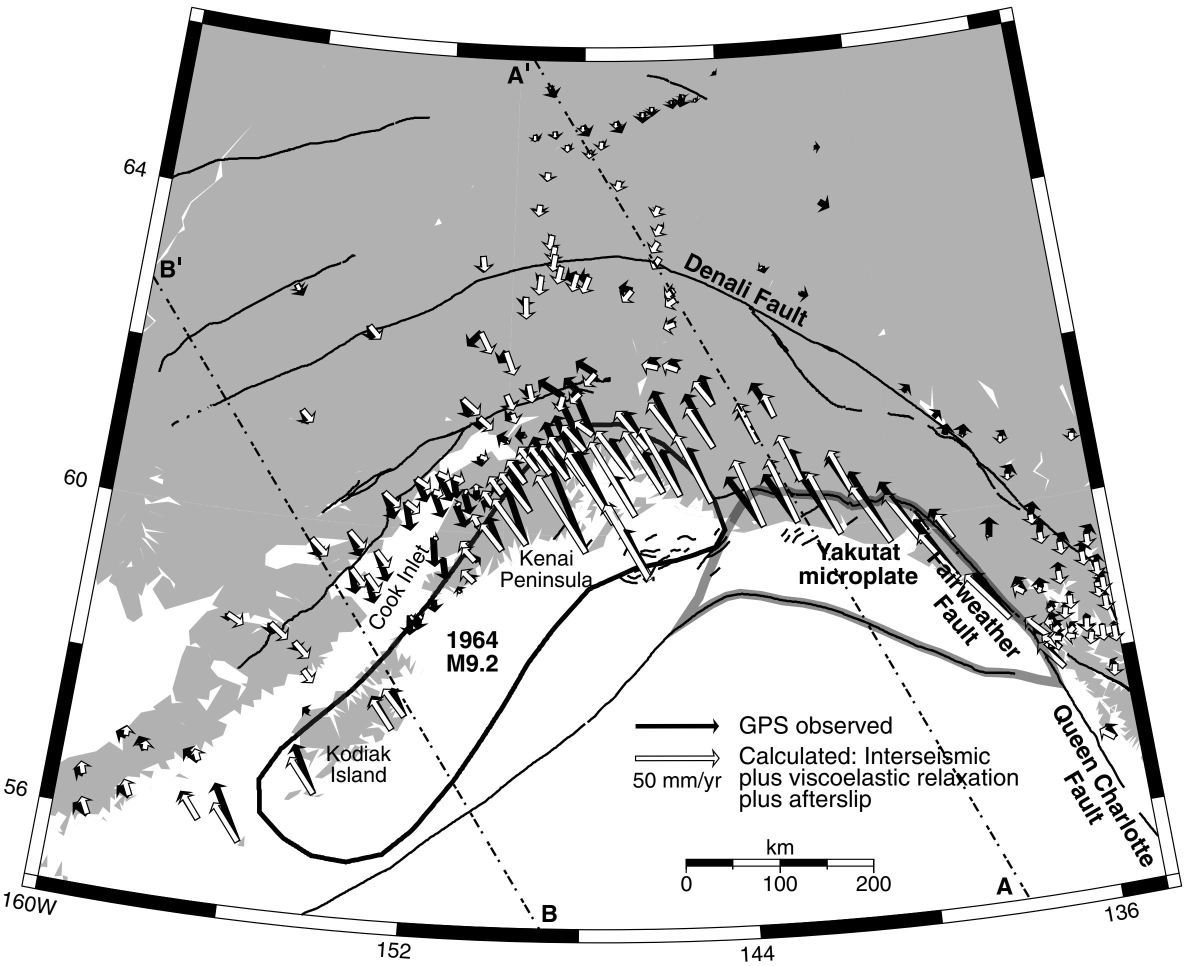

Figure 2. Average horizontal velocities in Alaska (w.r.t. stable North America) as observed by GPS from 1997 to 2002 and those calculated by a combined interseismic, viscoelastic relaxation and afterslip model (see text). Cross-section A–A' is where a 2-D model is used to explore interseismic deformation across the Yakutat microplate. Cross-section B–B' is where a 2-D model is used to explore interseismic and postseismic deformations across the 1964 Alaska earthquake rupture zone. GPS velocities are from Freymueller *et al.* (2008). For clarity, only a subset of the GPS velocities are shown.

is not influenced by post-seismic processes, perhaps explaining why Bufe's (2006) model cannot explain southward-directed velocities observed to the north of the Denali Fault.

Zweck *et al.* (2002) used 3-D elastic models to explain contemporary GPS velocities in the region surrounding the 1964 Alaska earthquake rupture zone and attributed the trenchward trending velocity vectors on Kenai Peninsula and near Cook Inlet to transient post-seismic afterslip following the 1964 earthquake. A similar conclusion has been suggested by Freymueller *et al.* (2000) using 2-D elastic models and a limited set of GPS data. A comparison between afterslip only models and GPS data in the region north of the Denali Fault, however, suggests that afterslip alone cannot be used to explain southerly directed velocity vectors in this far-field region

Transient post-seismic deformation following the 1964 earthquake has also been explained using 2-D (Sauber *et al.* 2006) and 3-D viscoelastic models (Suito & Freymueller 2009) that also account for viscous relaxation of lower crust/upper mantle in addition to afterslip. Suito & Freymueller (2009) found that a combination of viscoelastic relaxation, afterslip and interseismic elastic deformation is needed to explain the southeastward trending GPS velocities in the region just above and inland of the 1964 rupture. Their analysis, however, was limited to this region and did not consider the region to the east, where the plate boundary transitions from subduction to strike-slip faulting. Three $M > 7.5$ earthquakes have occurred since 1949 in this region, potentially generating a post-seismic component to the velocity field. These earlier studies also did not consider how deformation due to these various processes influences the evolution of crustal stress in the region.

Here we seek to understand the relative contributions of interseismic and post-seismic processes to the contemporary velocity field in central and southern Alaska, then use this knowledge to calculate interseismic stressing rates as well as the evolution of stress due to coseismic slip and post-seismic processes associated with the 1964 Alaska quake and the last three major earthquakes on the Fairweather and Queen-Charlotte faults. These processes are influenced by a wide variety of factors including the geometry of the Pacific/North American plate interface, which varies from shallow to deeply slipping along a strike that curves significantly (Fig. 1), the locking depth of the megathrust and the rheology of the lower crust and upper mantle. To this end we develop a numerical viscoelastic model that can consider these complexities and use it to determine the set of interseismic and post-seismic parameters required to explain the contemporary surface velocity field. Our stress evolution calculations concentrate on questions such as the magnitude and orientation of stresses transferred inland from the plate boundary to drive motion on the Denali Fault and how the evolution of transient stresses may have influenced the 2002 Denali earthquake.

2 ANALYSIS APPROACH

2.1 Model development

Our analysis utilizes several numerical models, one that considers the full 3-D geometry and mechanical behaviour of the Pacific–Alaskan margin, and two 2-D models that cut across the Yakutat microplate and across the 1964 rupture surface (Fig. 3). The discretized geometry for all models was generated using the Cubit toolkit (http://cubit.sandia.gov). The 3-D mesh contains ∼0.25 million elements that were necessary to characterize shallow subduction and the plate boundary transition from strike-slip faulting to normal subduction beneath Yakutat. The longitudinal model domain extends ∼1700 km in all four directions from a point centred at 60N latitude and 148W longitude, and to the base of the upper mantle at a depth of 670 km. The 2-D meshes contain ∼2000 elements and also extend to the base of the upper mantle. These models enable us to explore interseismic and post-seismic modelling approaches and parameter space in an efficient manner, enabling a more narrow focus with the computationally expensive 3-D calculations. The 2-D model that passes through the Yakutat microplate (Fig. 3b) enables us to look at different approaches to modelling interseismic deformation as this region appears to be outside of the areas 'significantly'

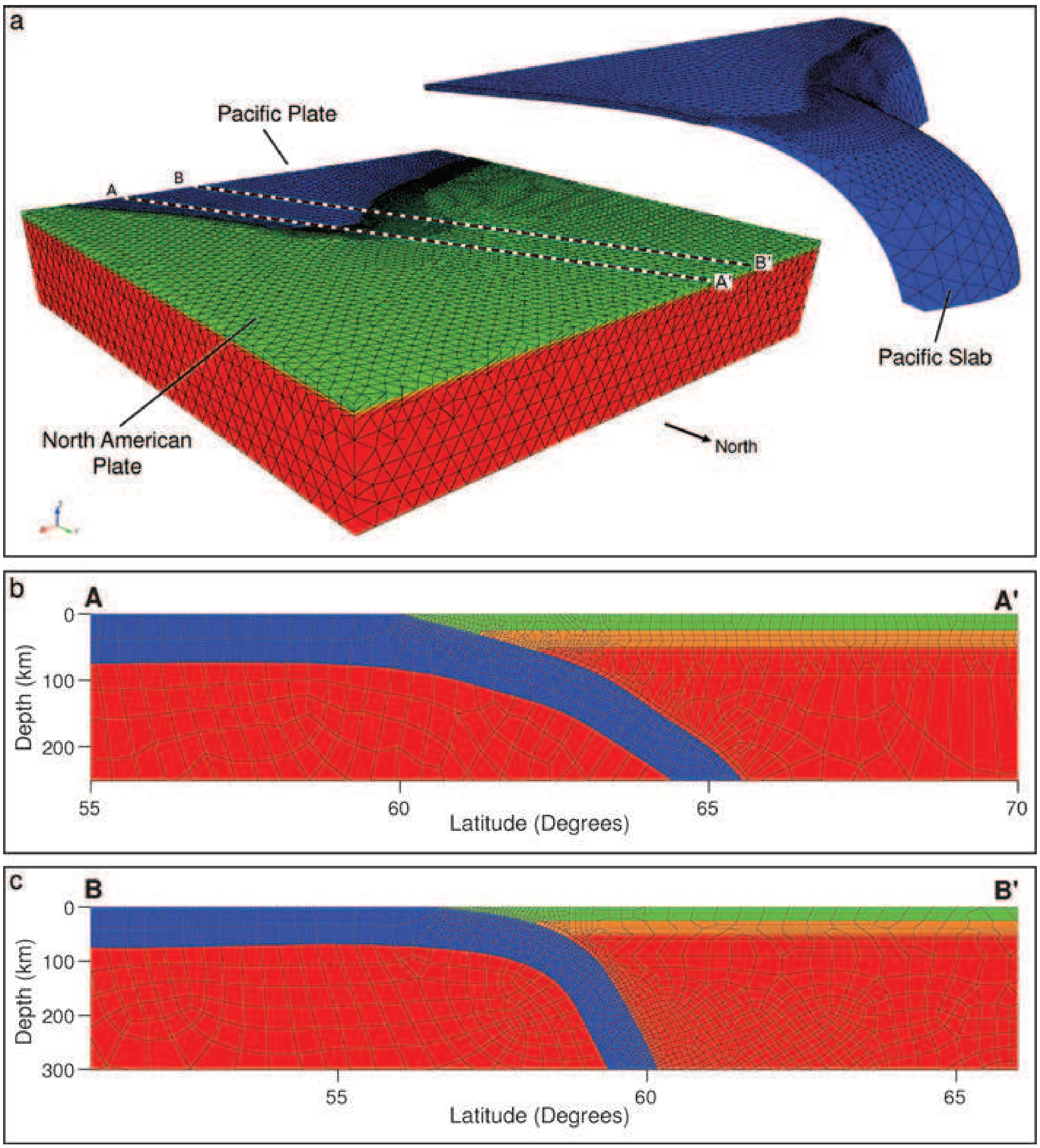

Figure 3. Finite element meshes used in this study. (a) Full 3-D model with slab geometry shown in inset. (b) Part of the 2-D mesh used for interseismic calculations through cross-section A–A' in Fig. 2. (c) Part of 2-D mesh used for interseismic and postseismic calculations through cross-section B–B' in Fig. 2. The actual meshes for (b) and (c) extends a few hundred kilometres on all three sides. The continental (in green) and oceanic crust (in blue) have a shear modulus of 39 and 52 GPa, respectively. The shear modulus for the mantle (red) is assumed to be 69 GPa. Poisson's ratio for all materials is assumed to be 0.25.

Table 1. Rupture parameters for all the earthquakes in the 3-D model; QCI, Queen-Charlotte Island; PWS, Prince William Sound; [∗] For the 1964 earthquake a variable slip model (with a uniform slip of 12 and 5 m on the Kodiak and Kenai asperities, respectively) has also been considered; [1] Nishenko & Jacob (1990); [2] Johnson *et al.* (1996).

Event year (location)	Magnitude (M_w)	Geometry (km × km)	Ave. dip-slip (m)	Ave. strike-slip (m)	Ref.
1949 (QCI)	8.1	400 × 15	0.0	5.8	[1]
1958 (Lituya Bay)	7.8	225 × 15	0.0	4.8	[1]
1964 (PWS)	9.2	740 × 250	8.6*	0.0	[2]
1972 (Sitka)	7.6 (M_s)	200 × 15	0.0	5.0	[1]

influenced by recent earthquakes (1964 Alaska earthquake to the west and the strike-slip earthquakes in the east). The 2-D model that passes through the 1964 rupture surface (Fig. 3c) incorporates GPS stations where surface velocities are directed to the southeast, presumably due to post-seismic processes associated with the 1964 rupture.

The design and implementation of the models are based on a number of assumptions and observational constraints. The north, west and eastern model boundaries are held fixed, which does not influence model results in mainland Alaska in the time frame of our analyses (1000s of years for models that consider several earthquake cycles). For runs that consider the motion of the subducting Pacific Plate over time, a velocity boundary condition is applied to the two ends of the slab, consistent with the motion of the Pacific Plate relative to North America in accordance with NUVEL-1A (DeMets *et al.* 1994). This velocity varies from ∼48 mm yr^{-1} at the eastern edge of the Yakutat microplate to ∼65 mm yr^{-1} at the western edge of the model domain. The approach can be described as a combined kinematic–dynamic description where the slab velocity is prescribed, but the flow of mantle surrounding the slab responds dynamically to slab motion. The advantage to this approach is that we do not have to worry about developing a Pacific slab that moves at the correct velocity based on a balance of density and viscosity, which is very difficult to achieve without consideration of global mantle circulation currents. Although velocity boundary conditions lead to inaccurate stresses within the slab, such stresses are not the objective of this analysis.

The geometry and extent of the slab is based on published slab contours and observed seismicity (Eberhart-Phillips *et al.* 2006). Although the plate boundary is well known along the Queen-Charlotte and Fairweather faults east of the Yakutat microplate and along the megathrust west of the Yakutat microplate, it is more diffused across the Yakutat microplate itself. This boundary may be in the process of transfer from the northern extent of the microplate to its southern edge as the microplate is currently being accreted onto the North American Plate. In general, the plate interface is locked in our simulations, so the exact location of the interface through the Yakutat microplate is not a critical factor.

The oceanic lithosphere is assumed to be 80 km thick and behaves elastically in all runs. An average thickness of 37.5 km for the continental crust is assumed, based on tomographic data of Eberhart-Phillips *et al.* (2006) and receiver function analysis of Veenstra *et al.* (2006). Although the crust varies from south of the Denali Fault (35–45 km) to northern lowlands (25 km) (Veenstra *et al.* 2006), its thickness is not a first-order parameter in our study. It is the strength of the lithosphere as a function of depth that primarily controls how the North American Plate responds to Pacific Plate convergence. For runs that only consider a single earthquake cycle, the effect of buoyancy forces is neglected. For runs that consider multiple earthquake cycles, buoyancy forces are included to prevent significant uplift/subsidence from occurring (on the free surface) over these longer time spans. The geometry and slip distribution for earthquakes is based after Nishenko & Jacob (1990) and Johnson *et al.* (1996) (Table 1). For the 1964 earthquake we use two models, one with uniform slip and the other with variable slip centred on two asperities on the Kodiak and Kenai segments of the megathrust (Holdahl & Sauber 1994; Johnson *et al.* 1996; Santini *et al.* 2003).

We assume a linear Newtonian viscoelastic rheology, which enables us to calculate separately and superimpose interseismic and post-seismic results. Transient surface displacement rates due to post-seismic relaxation following earthquakes have been inferred to be non-linear (e.g. Pollitz 2003, 2005; Freed & Burgmann 2004; Freed *et al.* 2006b). However, for this study we are looking at post-seismic velocities many decades after the events when displacement rates have slowed and behave in a more linear fashion. In addition, we only seek to understand average velocities across the GPS observational time period (1997–2002). Where an assumption of a linear viscosity may prove to be an impediment is when we explore spin-up models (described in Section 2.2) that require the calculation of the cumulative post-seismic response resulting from numerous earthquake cycles.

The viscosity structure of the lower crust and mantle wedge has been inferred from GPS observations of post-seismic relaxation following the 2002 Denali earthquake. The most appropriate study would be the power-law study of Freed *et al.* (2006b), as it estimates the magnitude of the longer-term (interseismic) viscosity structure of the lower crust and mantle wedge after the non-linear portion of a transient phase has diminished. This study suggested a mantle viscosity below 80 km of order (1–3) × 10^{19} Pa s and a mantle viscosity above 80 km depth of order (3–5) × 10^{19} Pa s, and a moderately stronger (10^{20} Pa s) lower crust. These values are similar to the 2.5 × 10^{19} Pa s inferred for the upper mantle by Hu *et al.* (2004) based on GPS observations many decades after the 1960 M9.5 Chilean earthquake and also to the 3.0 × 10^{19} Pa s as inferred by Suito & Freymueller (2009). Our analyses consider a variety of viscosity structures, with these previous studies serving as a guide as to what we should expect to find in this study.

2.2 Approaches to interseismic calculations

Interseismic deformation rates have been numerically simulated using a number of different approaches. One approach is the backslip model (Savage 1983), where virtual negative slip equal to the magnitude of the plate velocity is imposed on the locked segment of the active fault (Fig. 4a inset). For subduction zone settings, backslip with an appropriate locking depth for the megathrust can reproduce observed surface velocities on the overriding plate, but not for

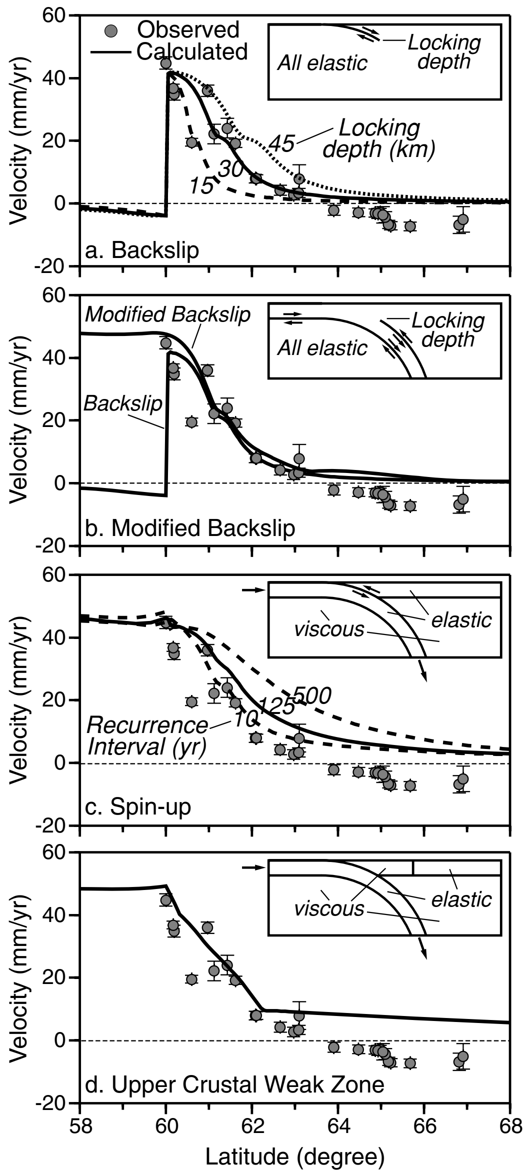

Figure 4. Comparison of GPS observed versus calculated horizontal surface velocities (+/– 25 km on either side) along a cross-section that passes through the Yakutat microplate (A–A' in Fig. 2; mesh shown in Fig. 3b) for a variety of approaches to modeling interseismic deformation. Illustrations of each approach are shown as insets in the respective panels. (a) Results for a backslip model as a function of several assumed locking depths. (b) Results for a modified backslip model for a depth of 30 km (backslip model shown for comparison). (c) Results for a spin-up model for various assumptions of the average earthquake recurrence interval. All spin-up models assume a lower crust and upper mantle viscosity of 1.5×10^{19} Pa s. (d) Results for a model that assumes a weak upper crustal zone of weakness between 60 and 62N.

the subducting plate and requires addition of a step function. An improved model proposed by Zhao & Takemoto (2000) (hereafter referred as the modified backslip model) in which slip is imposed below the locked portion of the interface, and at the base of the down-going slab (Fig. 4b inset) gives correct velocities for both the overriding plate as well as the subducting plate without the need of further processing (i.e. the addition of the step function). A similar approach has been used to model interseismic deformation in Sumatra by Sieh *et al.* (1999) and by Bufe (2006) for Alaska. From a computational standpoint, backslip and modified backslip models only require the solution of the elastic problem to determine an instantaneous interseismic velocity field.

Interseismic deformation rates have also been approximated using spin-up models where interseismic surface velocities are thought to be a cumulative effect of post-seismic relaxation following a number of previous earthquake cycles (e.g. Hetland & Hager 2006) (Fig. 4c inset). The idea is that the post-seismic stresses in the lower crust and upper mantle are not fully relaxed before the occurrence of the next earthquake. As a result, a small relaxation component remains that adds to the post-seismic process in the next earthquake cycle and so on, leading eventually to a long term, steady-state velocity component from previous events. This component adds to that induced by long-term plate motions, and after enough earthquake cycles, a new interseismic velocity structure emerges. Such a velocity field is simulated by running a number of earthquake cycles until the velocity structure within each cycle tracks like the previous cycle. Such models are said to have been spun-up. Since post-seismic velocities are generally greatest in the vicinity of the active fault, this process leads to higher interseismic surface velocities to concentrate near the fault, as observed near the megathrust in Alaska. The degree to which spinning up a model will localize surface velocities near an active fault is dependent on the viscosity structure and recurrence interval assumed. Non-linearity's in viscosity with time could greatly influence the resulting interseismic velocity field by accelerating relaxation rates early in an earthquake cycle, while decelerating later relaxation rates compared to a Newtonian rheology.

Finally, interseismic deformation rates can be modelled by consideration of a lateral zone of weak upper crust that accommodates more strain then surrounding regions (Fig. 4d inset). Such zones may be a consequence of damage or material heterogeneity resulting from thermo-mechanical effects. These zones have been modelled using a viscoelastic rheology where the viscosity is low enough such that a portion of the upper crust does not behave elastically (e.g. 10^{22}–10^{23} Pa s), but is a few orders of magnitude higher than lower crustal and upper mantle viscosities (e.g. Choi & Gurnis 2003; Yang *et al.* 2003; Platt *et al.* 2008). The use of a viscoelastic rheology is a means to simulate both elastic and anelastic deformations in the crust.

Our analysis approach is to initially explore the various methods for simulating interseismic deformation in southern Alaska using the 2-D model to guide us towards the best approach to use with the 3-D model. We similarly use the 2-D model to explore parameter space associated with post-seismic relaxation and afterslip processes to guide us towards the models that are going to likely work best in 3-D. 2-D calculations are accomplished using GeoFEST (Parker *et al.* 2008), a numerical code that solves the quasi-static momentum equation in a viscoelastic medium using the finite element method. Slip on faults is imposed using the split node method (Melosh & Raefsky 1981) that conceptually adds additional terms to the force vector leaving the stiffness matrix unchanged and the linear system of equations for the 2-D problem is solved using a direct solver. For 3-D calculations we use PyLith (Aagaard *et al.* 2008, 2009), an open source implicit/explicit finite element code for quasi-static and dynamic problems. In PyLith, slip on faults is accommodated by zero volume cohesive cells and is a constraint that is enforced using Lagrange Multipliers. The resulting indefinite system is solved using a parallel sparse direct solver.

3 RESULTS

3.1 2-D interseismic models

We initially explore how the backslip, modified backslip, spin-up and weak zone models work to explain observed surface velocities along a 2-D cross-section passing through the Yakutat microplate (Cross-section A–A' in Figs 2 and 3b). This is a region where velocities are thought to be controlled primarily by interseismic processes. Fig. 4(a) shows how GPS observed horizontal velocities compared with those calculated by the backslip approach based on three assumptions of locking depth (15, 30 and 45 km). A model with a 30 km locking depth appears to provide a better match to observed velocities on the North American Plate (north of 60N) than other models. This value is similar to the ∼30 km locking depth inferred from the observed depth of seismicity along the megathrust. The modified backslip model provides a very similar result to that of the backslip model, with the exception that it can account for the motion of the Pacific Plate (Fig. 4b) without the need of further processing. We would like to point out that there are a few stations along this cross-section north of 62N which have negative velocities that are a consequence of post-seismic viscous relaxation (discussed later) following the 1964 earthquake. This cross-section was chosen because it passes through a region that is less likely to be affected by post-seismic transients near the trench but in the far field (i.e. beyond 62N) some effects do show up.

For the spin-up approach we consider a variety of combinations of earthquake recurrence intervals and viscoelastic structures. An average recurrence time for earthquakes on the megathrust of order 500 years has been estimated from alternating beds of peat and mud in sediment sequences on the south-central Alaskan coast (Shennan & Hamilton 2006). If we initially consider a recurrence interval of 500 years in combination with a lower crust and upper mantle viscosity of 1.5×10^{19} Pa s, we find that predicted velocities with distance from the plate boundary are greatly over-estimated compared to those observed (Fig. 4c). To more closely simulate the observed drop-off of velocities inland, the recurrence interval must be lowered to ∼10 years, at which point a further decrease in recurrence time does not alter the solution. Such a recurrence interval for large megathrust events is, of course, unrealistic. A similar improvement of fit to the observed velocities can be achieved by increasing the viscosity of the lower crust and upper mantle to $\sim 10^{22}$ Pa s while keeping the recurrence interval at 500 years. But such a viscosity is several orders of magnitude higher than that inferred from the previous post-seismic studies discussed earlier. If the spin-up approach is in fact a reasonable characterization of the process by which interseismic velocity profiles form, it is plausible that the failure of this approach to work in our models resides in our assumption of linear Newtonian viscosities.

Finally, we use the 2-D model to test the weak upper crustal zone model. We assume a lower crustal and upper mantle viscosity of 1.5×10^{19} Pa s and a viscosity of 10^{22} Pa s for the weak zone of upper crust. The lateral extent of the weak zone can be determined from the drop-off in GPS observed velocities and corresponds to a region that extends from the megathrust to ∼62N (Fig. 4d). This approximately corresponds to where an extension of the Castle Mountain fault would lie to the east, although there is no observational evidence for such an extension. In addition, the weak upper crustal zone should experience significantly more permanent strain than regions to the north, which indeed is the case as the St. Elias Range which lies south of the supposedly eastern extension of the Castle Mountain fault does undergo rapid contraction. However, due to the difficulty of identifying such a boundary throughout Southern Alaska with absolute certainty especially when the GPS velocities are being influenced by transient processes this approach is not feasible. These 2-D results suggest that the modified backslip model works best for calculating interseismic deformation, especially for computationally expensive 3-D models.

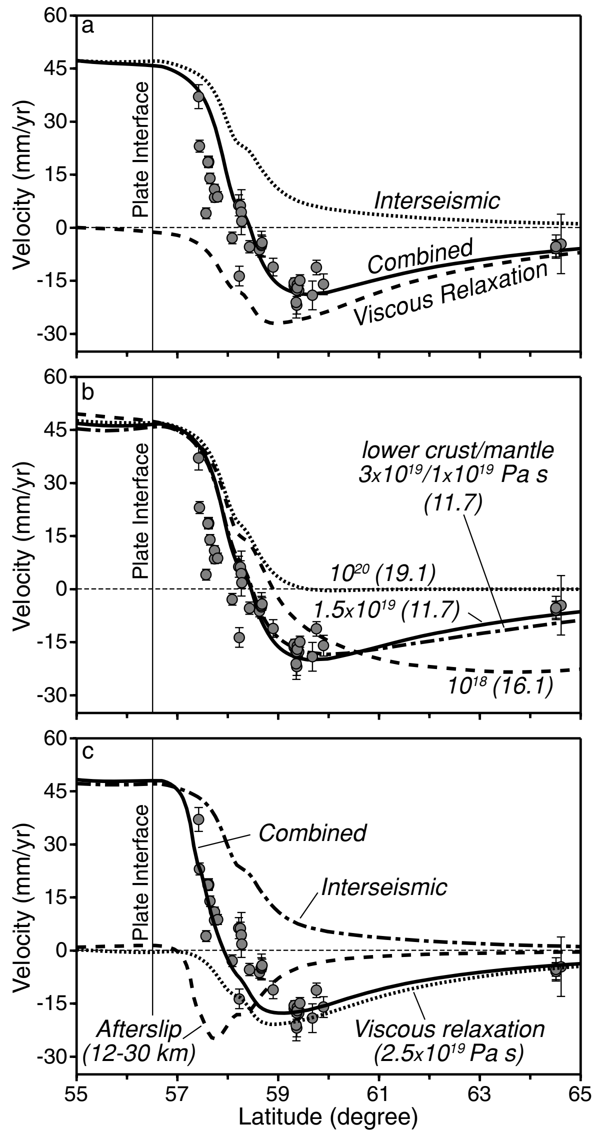

Figure 5. Comparison of GPS observed versus calculated horizontal surface velocities along a cross-section that passes through the 1964 Alaska rupture surface (B–B' in Fig. 2; mesh shown in Fig. 3c). (a) Component and combined results of a model consisting of viscous relaxation (1.5×10^{19} Pa s lower crust and mantle viscosity) and interseismic deformation (modified backslip with a 30 km locking depth). (b) Variation of the combined model in (a) as a function of the assumed viscosity structure. The number in bracket shows the misfit value for the residual velocities (i.e. sqrt$[(1/n)\sum(v_o - v_m)^2]$ where v_o and v_m are the observed and modelled velocities respectively and n the number of observation points). Unless otherwise stated, viscosity shown is that of the lower crust and mantle. (c) Component and combined results of a model consisting of viscous relaxation (2.5×10^{19} Pa s lower crust and mantle viscosity), afterslip (55 mm yr^{-1} from 13 to 30 km depth) and interseismic deformation (modified backslip a with 30 km locking depth).

3.2 2-D post-seismic models

For calculations of viscoelastic relaxation following the 1964 earthquake we utilize the 2-D model that incorporates the geometry of the Pacific and North American plates that passes through the 1964 rupture zone (cross-section B–B' in Figs 2 and 3c) near eastern Kodiak Island. Average contemporary velocities for the GPS observational time period (1997–2002) are calculated by applying slip associated with the 1964 rupture, then allowing the viscoelastic structure to relax for 36 years (∼2000). The bottom and side boundaries of the domain for this model remain fixed. A uniform slip of 7.5 m that extends to a depth of 30 km (Johnson *et al.* 1996) is applied along the interface. If we initially assume a uniform viscosity for the lower crust and upper mantle as 1.5×10^{19} Pa s, we calculate a contemporary horizontal velocity profile as shown by the dashed line in Fig. 5(a). The profile shows viscous relaxation to lead to southerly directed velocities (negative velocities in the figure) several hundred kilometres inland from the plate boundary. When we add the viscous relaxation velocity profile to one calculated for interseismic motion (using the modified backslip model with a 30 km locking

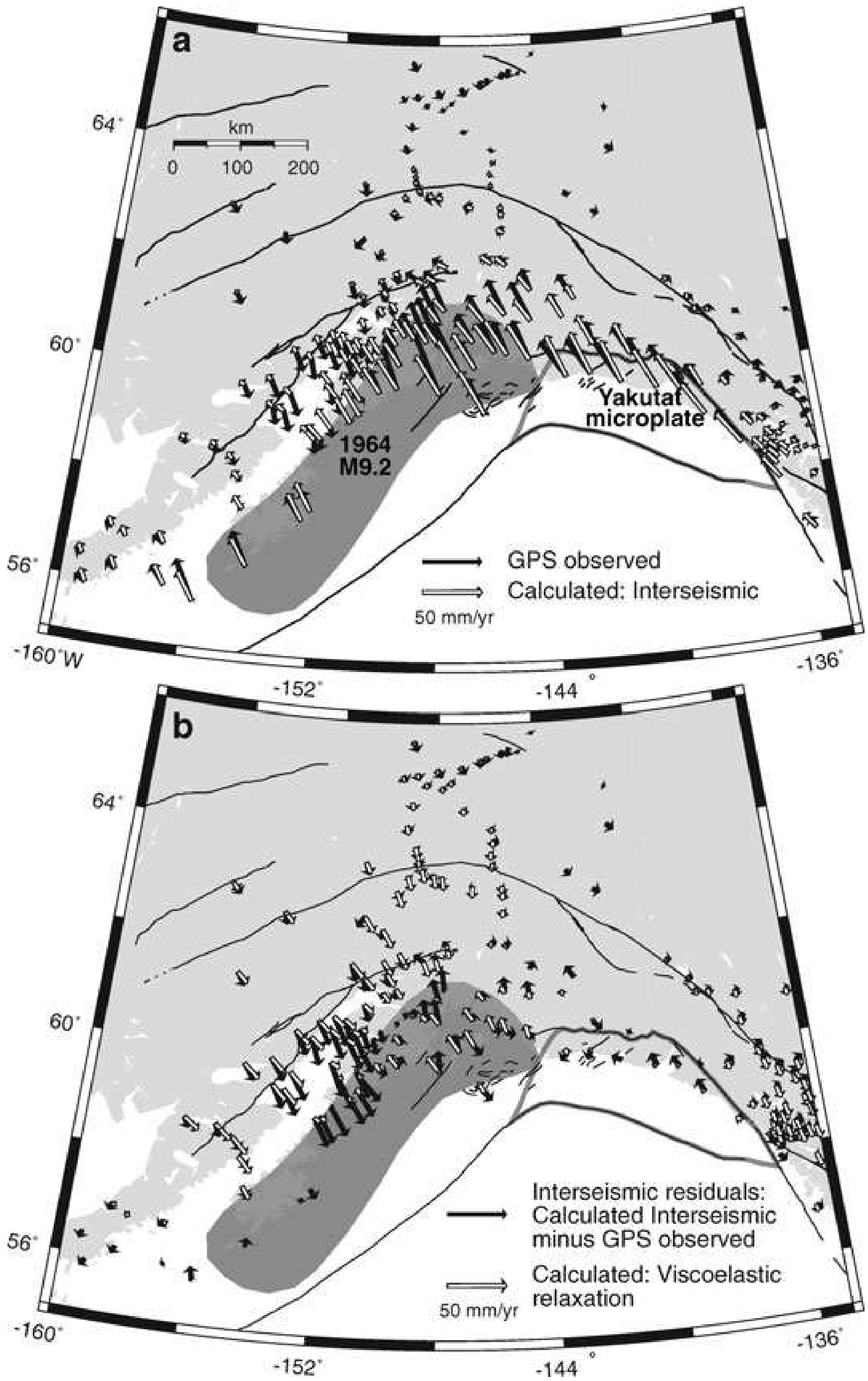

Figure 6. (a) Comparison of GPS observed versus calculated horizontal surface velocities based on a model of interseismic deformation using a modified backslip model. (b) Comparison of residual velocities (GPS observed minus interseismic deformation) versus calculated velocities based on viscoelastic relaxation. (c) Comparison of residual versus calculated velocities based on viscoelastic relaxation plus afterslip. See text for model details.

depth), the calculated cumulative profile reasonably matches the observed GPS velocities along this cross-section, except close to the plate interface (∼57.5N), where velocities are more slower than this model would predict.

Fig. 5(b) shows how the predicted cumulative (interseismic plus viscous relaxation) velocity profile varies as function of assumed viscosity structure. A model in which the lower crust and upper mantle has an average viscosity of 1.5×10^{19} Pa s provides the best fit, with higher and lower assumed viscosities leading to poor velocity fits both in the near and far-field. The observed velocities can also be explained by a viscosity structure where the lower crust has a viscosity three times that of the upper mantle (3×10^{19} compared to 1×10^{19} Pa s). Such a model would be more consistent with a decrease in viscosity with depth found in several post-seismic studies following the 2002 Denali earthquake (Pollitz 2005; Freed *et al.* 2006a).

The inability of the post-seismic relaxation model to explain slower velocities closer to the plate interface suggests that either the assumed rheology is in error or another mechanism such as afterslip is active. It is also possible that the velocity field near this cross-section is influenced by 3-D effects, but the 3-D results discussed in the next section show this to not be the case. Suito & Freymueller (2009) used observations of uplift to show that afterslip is the dominant mechanism active in the decades immediately after the 1964 earthquake, although forms a much diminished component of the contemporary velocity field. We find that we can add an afterslip component to that of viscous relaxation and interseismic deformation in our 2-D model (Fig. 5c) to achieve an improved fit compared to a model with only viscous relaxation and interseismic components. Afterslip in this model is simulated with a local Pacific Plate velocity at the cross-section of 55 mm yr^{-1} applied from 13 to 30 km depth. Other afterslip possibilities were considered, including slip closer to the surface and further down-dip. However, these models led to a poorer fit to the observed velocity field. Afterslip causes velocities close to the plate boundary to point south in a manner that cannot be achieved by viscous relaxation, whereas viscous relaxation causes velocities to point southwards farther from the plate boundary that afterslip cannot achieve (Fig. 5c). The best-fit three-component model requires a modestly higher viscosity structure (2.5×10^{19} Pa s) than the best-fit model without afterslip, indicative of the partial trade-off between afterslip and viscous relaxation processes. Because the magnitude of the afterslip required to fit the data is close to the plate velocity it is also possible that part of the megathrust between 13 and 30 km is not locked as is originally assumed but creeps at steady state. Such a low locking depth however cannot explain the slip distribution observed at this segment during the 1964 earthquake.

3.3 3-D calculations of the contemporary velocity field

Guided by the 2-D modelling results, we now use the 3-D model to understand the broad response of the Alaskan lithosphere to coseismic, post-seismic and interseismic processes. For the interseismic model we use the modified backslip approach, as it enables the most direct means of accurately generating the interseismic velocity field. For the 3-D model this means imposing slip on all of the edges of the Pacific slab consistent with observed plate motions, and assumed locking depths. A locking depth of 15 km along the strike-slip faults (consistent with empirical scaling laws), and 30 km along the megathrust (except for the Shumagin Gap (Fournier & Freymueller 2007) where it is known to transition to ∼5 km) as previously used in the 2-D models, has been assumed. Model results show a good fit to GPS observations in regions not significantly influenced by post-seismic processes (Fig. 6a). The interseismic only model explains well the GPS observations of higher velocities near the Yakutat coast and on Kodiak Island and west of this region. It also matches the counter-clockwise rotation of the velocity field just south of the Denali Fault, an indication of how subduction of the Pacific Plate drives inland shear taken up by this fault.

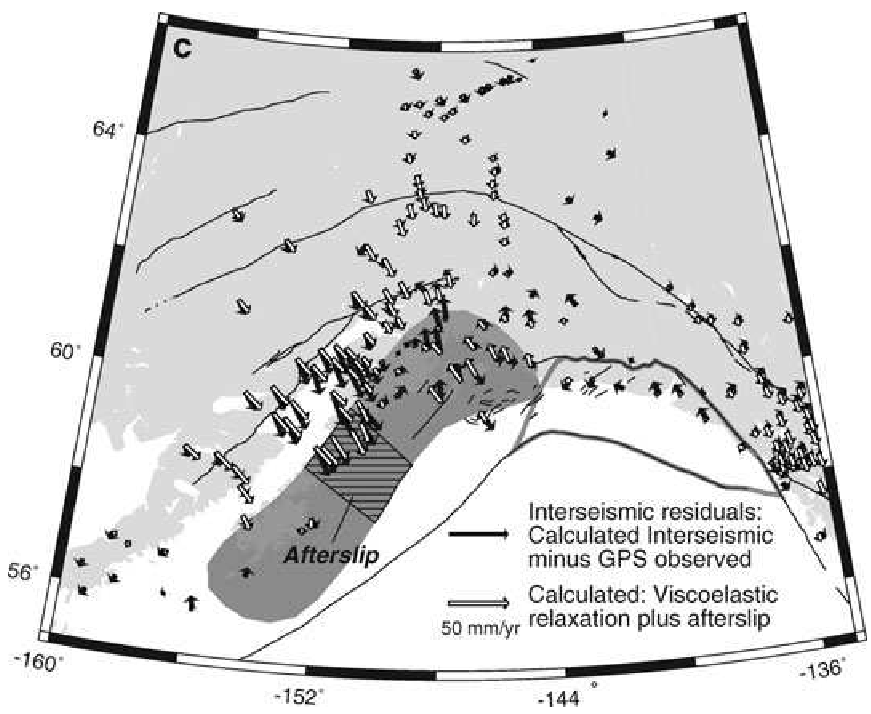

Figure 6. – *continued*.

The interseismic model cannot explain southwardly directed velocities near the Cook Inlet region and north of the Denali Fault. Nor can this model explain northwest trending velocities to the east of the Fairweather and Queen-Charlotte faults. These deficiencies are more easily observed by plotting the interseismic residuals, that is GPS observed minus calculated interseismic velocities (black arrows in Fig. 6b). The systematic pattern of trenchward directed residual velocities near the rupture zone of the 1964 Great Alaska earthquake is strongly suggestive of a post-seismic process. Likewise for small southeastwardly directed residual velocities just east of the Fairweather and Queen-Charlotte faults considering the proximity of the 1949, 1958 and 1972 events.

To study the influence of post-seismic relaxation following these four historic earthquakes, we simulated the slip of each event (Table 1) in a time consistent fashion and calculated predicted surface velocities in the year 2001. For the 1964 slip distribution we considered two models, one with uniform slip and one based on the two patch model with slip on the Kodiak and Kenai segments of the megathrust (Johnson *et al.* 1996). We found that post-seismic results associated with the 1964 earthquake were not significantly influenced by the choice of slip distribution as long as the moment magnitude of the event was similar in both representations. The calculations shown in the later sections are based on the two patch model of the 1964 earthquake. The calculated post-seismic relaxation velocities associated with a model that assumes a lower crustal viscosity of 3×10^{19} Pa s and a mantle viscosity of 1×10^{19} Pa s provide a good fit to interseismic residual velocities (Fig. 6b). Just like the 2-D model, an equivalent result is found when a viscosity of 1.5×10^{19} Pa s for the lower crustal and mantle is assumed. In general, the interseismic residuals are well explained by viscoelastic relaxation, especially in the region north of the Cook Inlet as well as inland north of the Denali Fault. The relaxation model poorly fits the interseismic residuals near the north and western edges of the Kenai Peninsula (Fig. 6b) as magnitude of the modelled velocities is significantly smaller than the residuals.

The region between Kodiak Island and the Kenai Peninsula happens to correspond to a region that accommodated minimal slip between slip patches in the two patch model suggested by Johnson *et al.* (1996). This region, shown as a hachured area within the 1964 rupture surface in Fig. 6(c), may be responding to coseismic stress changes associated with slip on the neighbouring patches. If we assume that this region is currently slipping at about the rate of Pacific Plate convergence and add the resulting afterslip surface velocities to that of the viscoelastic relaxation model, we find that the combined velocities provides an improved fit to the interseismic residual velocities (Fig. 6c) as the magnitudes are now correctly estimated. We found we could also achieve a similar improvement to fit to the original viscoelastic relaxation model if we decreased the viscosity of the lower crust in this region, which may be plausible owing to a potential increase in fluids within the lower crust from a dehydrating slab (Arcay *et al.* 2008; Billen & Gurnis 2001, 2003). Some misfit remains in the Cook Inlet region, perhaps because of our overly simplistic afterslip model. A more formal inversion for afterslip would likely have improved the model, but this was beyond the scope of this work.

Interpretation of interseismic residual velocities near the Fairweather and Queen-Charlotte faults is more difficult to understand. Southerly directed residual velocities in this region are explained by viscoelastic relaxation (Fig. 6b). But there are a number of residual velocities, most notably east of the Fairweather fault, which are directed to the northeast. There is no aspect of an interseismic, viscoelastic relaxation or afterslip calculation that could explain such velocity vectors. However, this region is currently being influenced by the world's fastest present day glacial unloading, which has been ongoing since the Little Ice Age (LIA) terminated around 1800–1850 (e.g. Sauber *et al.* 2000). LIA retreat is currently inducing more than 30 mm yr^{-1} of uplift centred in the Glacier Bay region (on the coast at ∼59N) (Larsen *et al.* 2004, 2005). The horizontal velocities associated with this process have not yet been determined, but one would expect a pattern in which these velocities would radiate out from the area, consistent with the northeastern directed velocities observed to the west. More work needs to be accomplished in this region once a post-glacial horizontal velocity component is established.

Calculated contemporary velocities based on a combined interseismic, viscoelastic relaxation and afterslip model are compared to those observed by GPS in Fig. 2. Overall there is good agreement between the observed and calculated velocity fields. Our results for the region surrounding the 1964 rupture zone are also in general agreement with that of Suito & Freymueller (2009). This demonstrates that, to a first order, contemporary surface velocities in Alaska can be explained as resulting from convergence of the Pacific Plate and transient post-seismic processes associated with recent (past 50 years) earthquakes in the region.

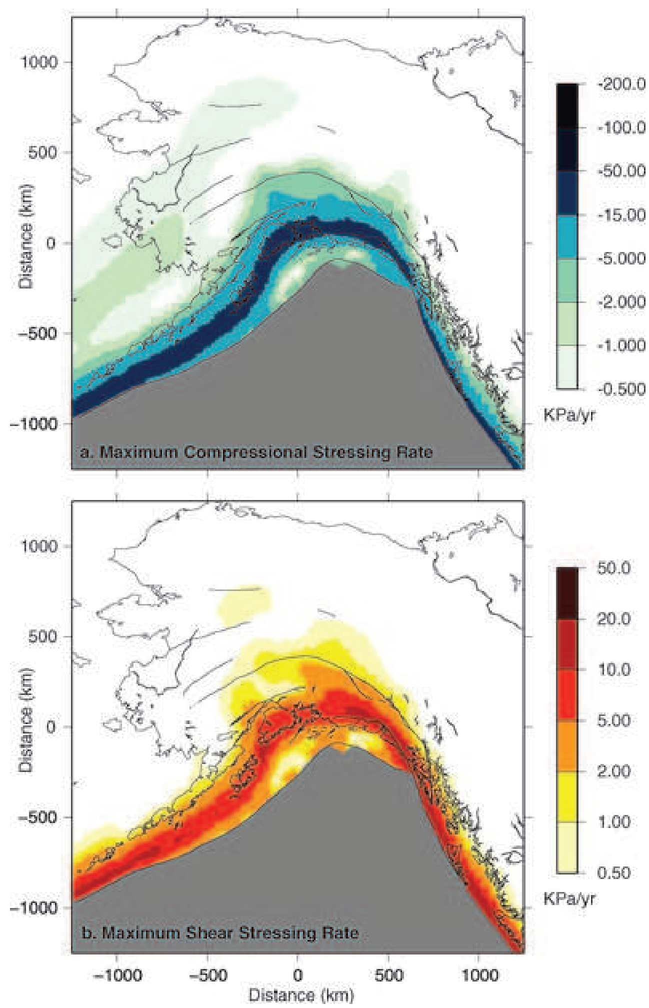

Figure 7. (a) Maximum compressive and (b) maximum shear stressing rates at the surface of the North American crust associated with the interseismic deformation.

4 STRESS EVOLUTION CALCULATIONS

Now that we have developed a 3-D numerical model that explains the contemporary velocity field, we use this model to calculate the evolution of stress over the past half century. We first consider how stressing rates in the Alaskan upper crust are influenced by the relative motion of the Pacific and North American plates. We then consider how stress has evolved on the major active fault systems due to interseismic, coseismic and post-seismic deformation.

Fig. 7 shows the calculated maximum compressive and maximum shear stressing rates in the upper North American crust associated with interseismic deformation. Inboard of the subduction zone, rates are greatest in a band located about ∼150 km from the plate boundary in the southwest, but about double that distance within the region of the Yakutat microplate. This is consistent with the location where GPS observed velocities were shown to experience a rapid drop-off. This zone of highest compressive and shear stressing rates lies directly above the location of the maximum locking depth, which extends further inland near Yakutat because of shallow subduction (Fig. 7). This result can be understood by examining the schematic of the modified backslip model (Fig. 4b, inset), which shows slip (opposing relative velocities of the slab and mantle wedge) applied starting at the base of the locked portion of the megathrust. The stress subsequently propagates to the crust that lies above. Maximum compressive normal stresses decrease to the south of this region (i.e. over the locked megathrust), as this region represents a zone in which stresses transition from the Pacific Plate (low stress due to slab pull) to the North American Plate (high stress due to convergence).

The zone of high shear stresses inboard of the subduction zone transitions to an even higher shear stress along the transform portion of the plate boundary (the Fairweather and Queen-Charlotte Fault system), where plate motion is directly associated with shear (Fig. 7b). The narrowness of the transform shear zone is consistent with the quickly diminishing magnitude of northwest trending observed velocities eastward from this fault system. Compressional stresses along this boundary (Fig. 7a) are a result of a modest azimuth difference between the strike of the Fairweather and Queen-Charlotte faults and the direction of the Pacific Plate relative to North America.

To understand how active faults are influenced by stresses through the earthquake cycle, we calculate changes in Coulomb stress. Coulomb stress calculations quantify how shear and normal stress changes act to push faults closer to (positive Coulomb stress change) or further away from (negative Coulomb stress change) failure (e.g. Jaeger & Cook 1979; Stein & Lisowski 1983; King *et al.* 1994; Freed 2005). Here we calculate the change in Coulomb stress,

$$\Delta\sigma_c = \Delta\tau - \mu'\Delta\sigma_n,$$

where $\Delta\tau$ is the change in shear stress parallel to the slip direction of a fault, $\Delta\sigma_n$ is change in fault-normal (or clamping) stress and μ' is the apparent friction, which takes into account reductions in friction due to pore pressure changes. Having no information on the

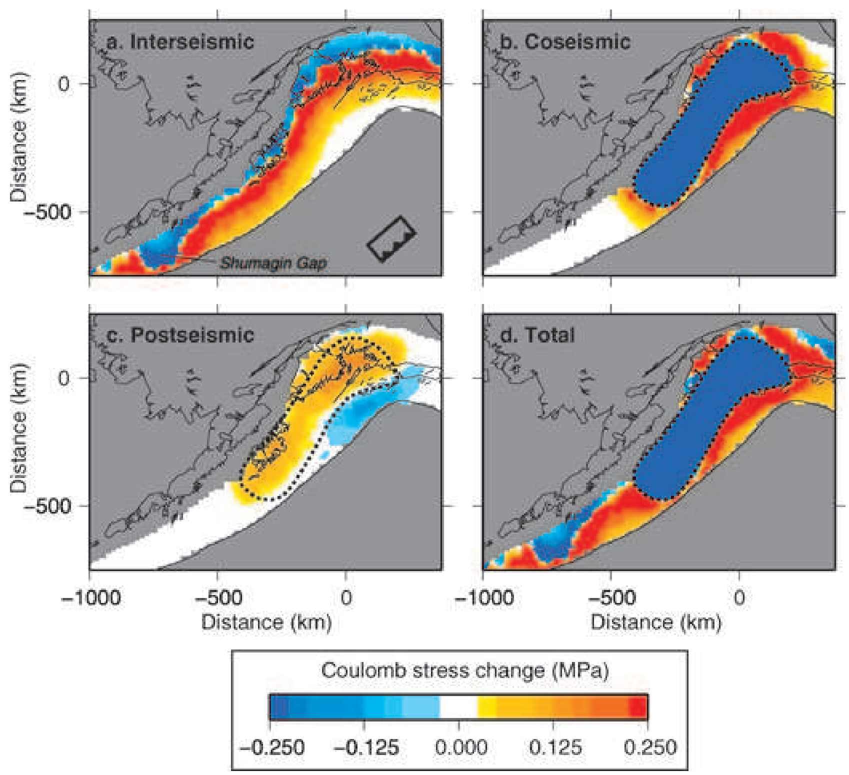

Figure 8. Coulomb stress change resolved on the Pacific megathrust from 1949 to 2002 due to (a) interseismic deformation, (b) coseismic slip, (c) postseismic viscoelastic relaxation and (d) interseismic plus coseismic slip plus viscoelastic relaxation. The Shumagin gap where the locked depth is inferred to be only ∼5 km deep is noted. The edge of the 1964 rupture surface is shown as a dashed line in (c). Coulomb stress change is calculated on thrust faults striking N47°E with a dip angle of 10°, based on an apparent friction coefficient of 0.1. Stresses on the megathrust are shown to a depth of 35 km, beyond which the dip angle is too steep for the calculated Coulomb stress component. Coseismic stress change on the 1964 rupture interface has been masked out in (b) and (d) (in dark blue).

absolute stress field, this calculation only considers how the stress field has evolved since a particular time.

We concentrate our Coulomb stress calculations on three of the most seismically active regions in Alaska: the megathrust along the plate interface, the Fairweather and Queen-Charlotte Fault system, and the central Denali fault. Fig. 8 shows calculated Coulomb stress changes resolved on the megathrust from 1949 (time of first earthquake considered) to 2002 (just before the Denali earthquake) due to the three components of the earthquake cycle, individually and combined. This figure shows results based on an assumed friction coefficient of 0.1, but these results are not significantly altered by other assumptions of friction, as the shear stress component is the dominant factor in the Coulomb calculation. The motion of the Pacific Plate is shown to load (warm colours) the locked megathrust towards failure (Fig. 8a). Coseismic slip then relieves stress on the two primary slip patches (blue regions) associated with the 1964 earthquake (Fig. 8b). Slip on these patches also causes an increase in Coulomb stress in surrounding fault regions. Coulomb stress increase between the slip patches was inferred to potentially have induced on-going afterslip, as discussed previously. Viscoelastic relaxation within the lower crust and mantle wedge serves to partially reload the slip patches as shown in Fig. 8(c). The cumulative stress change since 1949 suggests that the 1964 rupture surface has not yet recovered the stress drop associated with that earthquake, although stress has increased significantly in surrounding regions (Fig. 8d). It is possible that stress has relaxed in many of these regions, especially up-dip and between the two slip patches, due to aseismic slip, but this is difficult to verify due to the lack of off-shore geodetic constraints. The region along the megathrust to the west, between the 1964 rupture surface and the Shumagin gap (blue region in western part of Fig. 8d) and to the east near Yakataga, is the next likely region for large earthquakes.

Fig. 9 shows calculated Coulomb stress changes resolved on the Fairweather and Queen-Charlotte transform boundary from 1949 to 2002 due to the three components of the earthquake cycle and combined. Interseismic motion of the Pacific Plate is shown to load the locked boundary towards failure (Fig. 9a), while coseismic slip associated with the 1949, 1958 and 1972 relieves this stress along the entire length of the fault in this region (Fig. 9b). Viscoelastic relaxation within the lower crust and mantle then serves to partially reload the rupture surface and unload the region to the east (Fig. 9c). Note how both coseismic and post-seismic Coulomb stress changes along the Fairweather Fault serve to unload the southern continuation of the eastern Denali Fault, that is the Duke River–Dalton–Chatham faults, perhaps explaining why they are no longer active (Lahr & Plafker 1980). The cumulative stress change calculation suggests that the plate interface between Queen-Charlotte and Vancouver Islands (southeastern corner of Fig. 9d) has accumulated significant stress since 1949.

Fig. 10 shows calculated Coulomb stress changes resolved on the Denali Fault from 1949 to 2002 due to the three components of the earthquake cycle. Interseismic deformation is shown to increase Coulomb stress all the way from the plate interface to the Denali Fault (Fig. 10a), supporting the idea that the Denali fault is a result of partitioning of strain associated with oblique convergence of the Pacific Plate. Coseismic slip associated with the 1964 earthquake does not significantly influence Coulomb stress on the Denali Fault (Fig. 10b), but ∼4 decades of viscoelastic relaxation leads to an increase in Coulomb stresses along a major part of the fault that subsequently ruptured in 2002 (Fig. 10c). This demonstrates how post-seismic relaxation can influence faults hundreds of kilometres away from great earthquakes. The total stress change resolved on the Denali Fault shows it to be significantly loaded in the past 50 years leading up to the 2002 rupture (Fig. 10d). This increase in stress allowed the rupture, which originated in the west to propagate eastward with relative ease.

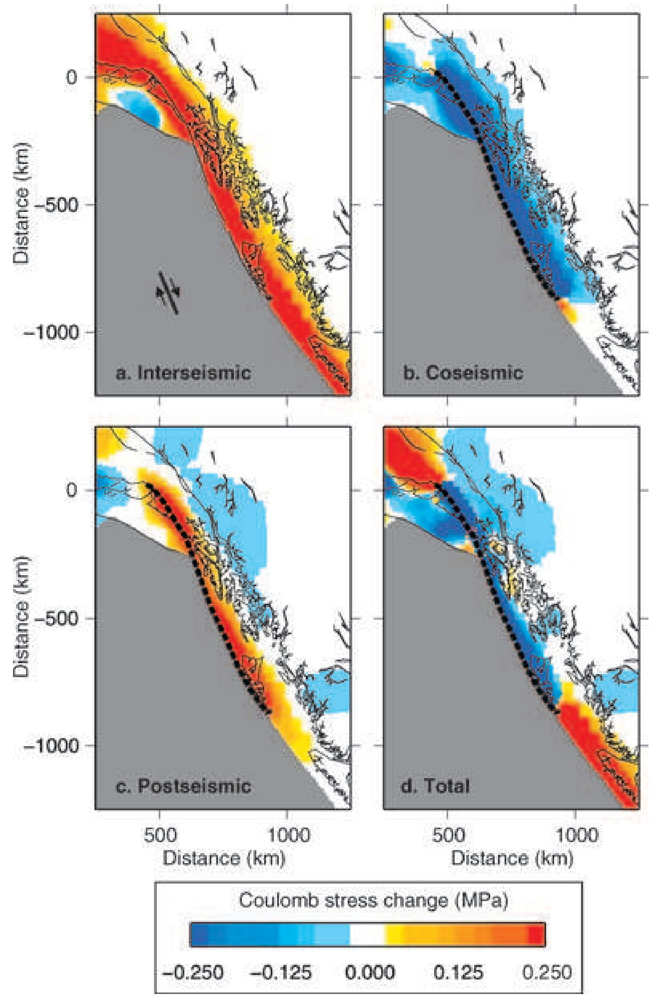

Figure 9. Coulomb stress change resolved on the Fairweather and Queen-Charlotte faults from 1949 to 2002 due to (a) interseismic deformation, (b) coseismic slip, (c) postseismic viscoelastic relaxation and (d) interseismic plus coseismic slip plus viscoelastic relaxation. The extent of the rupture surface of the 1949, 1958 and 1972 events on this transform boundary is shown as a black dashed line in (b–d). Coulomb stress change is calculated on vertical right lateral strike slip faults striking N70°E, based on an apparent friction coefficient of 0.1. Stresses are not recovered for the Pacific Plate, which is blacked out in the figures.

5 CONCLUSIONS

We have developed 2-D and 3-D numerical models to calculate how interseismic deformation due to relative plate motions, large earthquakes and post-seismic processes contribute to the contemporary velocity field and the evolution of the stress in the Alaskan crust. 2-D models show that interseismic deformation is best simulated using a modified backslip model, as Newtonian viscosity spin-up models cannot explain the rapid drop-off of northerly directed horizontal surface velocities with distance from the plate interface, and a weak zone of upper crust is not supported by geological

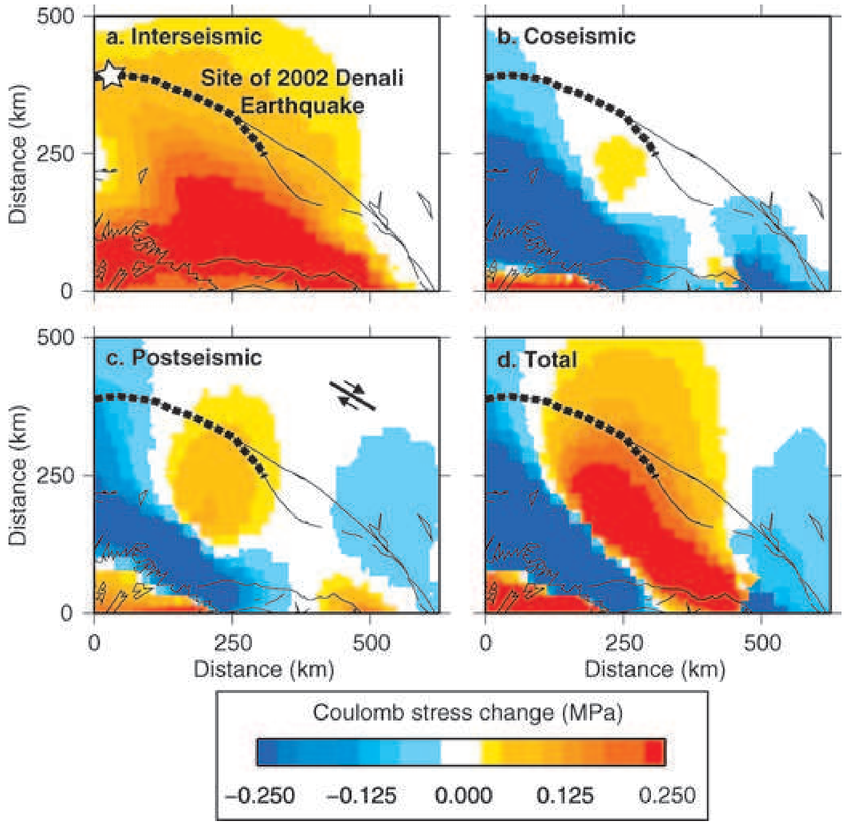

Figure 10. Coulomb stress change resolved on the central Denali Fault from 1949 to 2002 due to (a) interseismic deformation, (b) coseismic slip, (c) post-seismic viscoelastic relaxation and (d) interseismic plus coseismic slip plus viscoelastic relaxation. The rupture surface of the 2002 Denali earthquake (though not ruptured for this calculation) is shown as a bold dashed line. Coulomb stress change is calculated on vertical right lateral strike slip faults striking N30°E, based on an apparent friction coefficient of 0.1.

observations. Using the modified backslip approach, a 3-D model shows that northerly directed velocities can be explained by subduction of the Pacific Plate with a megathrust locked to a depth of 30 km. This model leads to interseismic velocities that drop off dramatically above the location of the maximum locking depth of the megathrust below. Flat subduction beneath the Yakutat microplate increases the width of the locking zone, pushing the region where interseismic velocities drop off further inland.

While northerly directed surface velocities within Alaska are well explained by the convergence of the Pacific Plate, southerly directed velocities require a separate process. Viscoelastic relaxation of the lower crust and upper mantle (order 10^{19} Pa s) following the 1964 Alaska earthquake works well to explain southerly directed velocities from the coast in the vicinity of the 1964 rupture zone to well north of the Denali Fault. This transient model cannot, however, explain observed southerly velocities very close to the rupture zone in a region that lies between the two primary slip patches of the 1964 earthquake. Afterslip within this region combined with post-seismic relaxation and interseismic deformation explains observed surface velocities within this region and throughout most of Alaska.

We use the 3-D model to calculate the evolution of stress in the Alaskan crust associated with interseismic deformation, coseismic slip associated with the 1964 megathrust earthquake and three events along the Fairweather and Queen-Charlotte faults (in 1949, 1958 and 1972), and viscoelastic relaxation associated with these events. Interseismic model results suggest that contemporary stressing rates, both compressional and shear, are greatest within a band of crust that overlies the down-dip edge of the locked portion of the megathrust. Because of shallow subduction beneath the Yakutat microplate, this increases the inland reach of high compression and shear stresses. Interseismic deformation is shown to load the megathrust and the transform plate boundary to the east. Interseismic deformation is also shown to load the Denali Fault, suggesting that this fault acts to partition strain associated with oblique subduction. Coseismic stresses are shown to relieve interseismic stresses along the megathrust, while loading the surrounding regions. Coseismic stresses along the transform boundary serve to relieve stresses on the fault as well as regions to the east. Post-seismic relaxation is shown to reverse the trend of coseismic stresses on the megathrust and surrounding regions, while on the transform fault post-seismic relaxation works to reload the fault but relieves stress to the east. Of particular interest is the result that post-seismic relaxation following the 1964 earthquake worked to load the rupture surface of the 2002 Denali earthquake several hundred kilometres inland.

ACKNOWLEDGMENTS

Reviews by Jeff Freymueller and two anonymous reviewers substantially improved the paper. This project was funded by NSF EAR Grant 0309620 and USGS NEHRP Grant 104266.

REFERENCES

Aagaard, B., Williams, C. & Knepley, M., 2008. PyLith: a finite-element code for modeling quasi-static and dynamic crustal deformation, *EOS, Trans. Am. geophys. Un.,* **89**(53), Fall Meet. Suppl., Abstract T41A-1925.

Aagaard, B., Kientz, S., Knepley, M., Strand, L. & Williams C., 2009. *PyLith User Manual,* v1.4, Computational Infrastructure of Geodynamics, Pasadena, CA. URL: www.geodynamics.org/cig/software/short/pylith/pylith_book-1.4.pdf.

Ali, S.T., Freed, A.M., Calais, E., Manaker, D.M. & McCann, W.R., 2008. Coulomb stress evolution in Northeastern Caribbean over the past 250 years due to coseismic, postseismic and interseismic deformation, *Geophys. J. Int.,* **174,** 904–918.

Arcay, D., Lallemand, S. & Doin, M.-P., 2008. Back-arc strain in subduction zones: statistical observations versus numerical modeling, *Geochem. Geophys. Geosyst.,* **9,** Q05015, doi:10.1029/2007GC001875.

Billen, M.I. & Gurnis, M., 2001. A low viscosity wedge in subduction zones, *Earth planet. Sci. Lett.,* **93,** 227–236.

Billen, M.I. & Gurnis, M., 2003. A comparison of dynamic models in the Aleutian and Tonga-Kermadec subduction zones, *Geochem. Geophys. Geosys.,* **4,** 1035, doi:10.1029/2001GC000295.

Bufe, C.G., 2006. Coulomb stress transfer and tectonic loading preceding the 2002 Denali fault earthquake, *Bull. seism. Soc. Am.,* **96,** 1662–1674.

Choi, E. & Gurnis, M., 2003. Deformation in transcurrent and extensional environments with widely spaced weak zones, *Geophys. Res. Lett.,* **30,** 1076, doi:10.1029/2002GL016129.

Cohen, S.C. & Freymueller, J.T., 2004. Crustal deformation in Southcentral Alaska: the 1964 Prince William sound earthquake subduction zone, *Adv. Geophys.,* **47,** 1–63.

DeMets, C., Gordon, R.G., Argus, D.F. & Stein, S., 1994. Effect of recent revisions to the geomagnetic reversal timescale on estimates of current plate motions, *Geophys. Res. Lett.,* **21,** 2191–2194.

Eberhart-Phillips, D. *et al*., 2003. The 2002 Denali Fault Earthquake, Alaska: a large magnitude, slip-partitioned event, *Science,* **300,** 1113–1118.

Eberhart-Phillips, D., Christensen, D.H., Brocher, T.M., Hansen, R., Ruppert, N.A., Haeussler, P.J. & Abers, G.A., 2006. Imaging the transition from Aleutian subduction to Yakutat collision in central Alaska, with local earthquakes and active source data, *J. geophys. Res.,* **111,** B11303, doi:10.1029/2005JB004240.

Freed, A.M., 2005. Earthquake triggering by static, dynamic, and postseismic stress transfer, *Ann. Rev. Earth planet. Sci.,* **33,** 335–367.

Freed, A.M. & Burgmann, R., 2004. Evidence of power-law flow in the Mojave Desert mantle, *Nature,* **430,** 548–551.

Freed, A.M., Ali, S.T. & Burgmann, R., 2007. Evolution of stress in Southern California for the past 200 years from coseismic, postseismic and interseismic stress changes, *Geophys. J. Int.,* **169,** 1164–1179.

Freed, A.M., Burgmann, R., Calais, E., Freymueller, J.T. & Hreinsdottir, S., 2006a. Implications of deformation following the 2002 Denali, Alaska earthquake for postseismic relaxation processes and lithospheric rheology, *J. geophys. Res.,* **111,** B01401, doi:10.1029/2005JB003894.

Freed, A.M., Burgmann, R., Calais, E. & Freymueller, J., 2006b. Stress-dependent power-law flow in the upper mantle following the 2002 Denali, Alaska, earthquake, *Earth planet. Sci. Lett.,* **252,** 481–489.

Freymueller, J.T., Cohen, S.C. & Fletcher, H.J., 2000. Spatial variations in present-day deformation, Kenai Peninsula, Alaska, and their implications, *J. geophys. Res.,* **105,** 8079–8101.

Fournier, T.J. & Freymueller, J.T., 2007. Transition from locked to creeping subduction in the Shumagin region, Alaska, *Geophys. Res. Lett.,* **34,** L06303, doi:10.1029/2006GL029073.

Freymueller, J.T., Woodard, H., Cohen, S.C., Cross, R., Elliott, J., Larsen, C.F., Hreinsdottir, S. & Zweck, C., 2008. Active deformation processes in Alaska, based on 15 years of GPS measurements, in *Active Tectonics and Seismic Potential of Alaska,* Geophysical Monograph Series, Vol. 179, Am. geophys. Un.

Hetland, E.A. & Hager, B.H., 2006. Interseismic strain accumulation: spin-up, cycle invariance, and irregular rupture sequences, *Geochem. Geophys. Geosyst.,* **7,** Q05004, doi:10.1029/2005GC001087.

Holdahl, S.R. & Sauber, J., 1994. Coseismic slip in the 1964 Prince William Sound earthquake: a new geodetic inversion, *Pure appl. Geophys.,* **142,** 55–82.

Hu, Y. Wang, K., He, J., Klotz, J. & Khazaradze, G., 2004. Three-dimensional viscoelastic finite element model for post- seismic deformation of the great 1960 Chile earthquake, *J. geophys. Res.,* **109,** doi:10.1029/2004JB003163.

Jaeger, J. & Cook, N., 1979. *Fundamentals of Rock Mechanics,* 3rd edn, Chapman and Hall, London.

Johnson, M., Satake K., Holdahl R. & Sauber J., 1996. The 1964 Prince William Sound earthquake: joint inversion of tsunami and geodetic data, *J. geophys. Res.,* **101,** 523–532.

Kanamori, H., 1997. The energy release of great earthquakes, *J. geophys. Res.,* **82,** 2981–2987.

King, G.C.P., Stein, R.S. & Lin, J., 1994. Static stress changes and triggering of earthquakes, *Bull. seism. Soc. Am.,* **84,** 935–953.

Khazaradze, G., Wang, K., Klotz, J., Hu, J. & He, J., 2002. Prolonged post-seismic deformation of the 1960 great Chile earthquake and implications for mantle rheology, *Geophys. Res. Lett.,* **29,** 2050, doi:10.1029/2002GL015986.

Lahr, J.C. & Plafker, G., 1980. Holocene Pacific–North American plate interaction in southern Alaska: implications for the Yakataga seismic gap, *Geology,* **8,** 483–486.

Larsen, C.F., Motyka, R.J., Freymueller, J.T., Echelmeyer, K.A. & Ivins, E.R., 2004. Rapid uplift of southern Alaska caused by recent ice loss, *Geophys. J. Int.,* **158,** 1118–1133.

Larsen, C.F., Motyka, R.J., Freymueller, J.T., Echelmeyer, K.A. & Ivins, E.R., 2005. Rapid viscoelastic uplift in southeast Alaska caused by post-Little Ice Age glacial retreat, *Earth planet. Sci. Lett.,* **237,** 548–560.

Melosh, H.J. & Raefsky, A., 1981. A simple and efficient method for introducing faults into finite element computations, *Bull. seism. Soc. Am.,* **71,** 1391–1400.

Nishenko, S.P. & Jacob, K.H., 1990. Seismic potential of the Queen Charlotte-Alaska-Aleutian seismic zone, *J. geophys. Res.,* **95,** 2511–2532.

Parker, J. *et al*., 2008. Geophysical finite-element simulation tool (GeoFEST): algorithms and validation for quasistatic regional faulted crust problems, *Pure appl. Geophys.,* **165,** 497–521.

Platt, J.P., Kaus, B.J.P. & Becker, T.W., 2008. The San Andreas Transform system and the tectonics of California: an alternative approach, *Earth planet. Sci. Lett.,* **274,** 380–391.

Pollitz, F.F., 2003. Transient rheology of the uppermost mantle beneath the Mojave Desert, California, *Earth planet. Sci. Lett.,* **215,** 89–104.

Pollitz, F.F., 2005. Transient rheology of the upper mantle beneath central Alaska inferred from the crustal velocity field following the 2002 Denali earthquake, *J. geophys. Res.,* **110,** B08407, doi:10.1029/2005JB003672.

Santini, S., Dragoni, M. & Spada, G., 2003. Asperity distribution of the 1964 Great Alaska earthquake and its relation to subsequent seismicity in the region, *Tectonophysics,* **367,** 219–233.

Sauber, J., Plafker, G., Molnia, B. & Bryant, M., 2000. Crustal deformation associated with glacial fluctuations in the eastern Chugach Mountains, Alaska, *J. geophys. Res.,* **105,** 8055–8077.

Sauber, J., Carver, G., Cohen, S. & King, R., 2006. Crustal deformation and the seismic cycle across the Kodiak Islands, Alaska, *J. geophys. Res.,* **111,** B02403, doi:10.1029/2005JB003626.

Savage, J.C., 1983. A dislocation model of strain accumulation and release at a subduction zone, *J. geophys. Res.,* **88,** 4984–4996.

Sieh, K., Ward, S.N., Natawidjaja, D. & Suwargadi, B.W., 1999. Crustal deformation at the Sumatran subduction zone revealed by coral rings, *Geophys. Res. Lett.,* **26,** 3141–3144.

Shennan, I. & Hamilton, S., 2006. Coseismic and pre-seismic subsidence associated with great earthquakes in Alaska, *Quaternary Sci. Rev.,* **25,** 1–8.

Stein, R.S. & Lisowski, M., 1983. The 1979 Homestead Valley earthquake sequence, California: control of aftershocks and postseismic deformation, *J. Geophys. Res.,* **88,** 6477–6490.

Stout, J.H. & Chase, C.G., 1980. Plate kinematics of the Denali fault system, *Can. J. Earth Sci.,* **17,** 1527–1537.

Suito, H. & Freymueller, J.T., 2009. A viscoelastic and afterslip postseismic deformation model for the 1964 Alaska earthquake, *J. geophys. Res.,* **114,** B11404, doi:10.1029/2008JB005954.

Veenstra, E., Christensen, D.H., Abers, G.A. & Ferris, A., 2006. Crustal thickness variation in south-central Alaska, *Geology,* **34,** 781–784.

Yang, Y., Liu, M. & Stein, S., 2003. A 3-D geodynamic model of lateral crustal flow during Andean mountain building, *Geophys. Res. Lett.,* **30,** 2093, doi:10.1029/2003GL018308.

Zhao, S. & Takemoto, S., 2000. Deformation and stress change associated with plate interaction at subduction zones: a kinematic modeling, *Geophys. J. Int.,* **142,** 300–318.

Zweck, C., Freymueller, J.T. & Cohen, S.C., 2002. Three-dimensional elastic dislocation modeling of the postseismic response to the 1964 Alaska Earthquake, *J. geophys. Res.,* **107,** doi:10.1029/2001JB000409.